

# Introduction of an electron push-pull system yields a planar *Red Kaede* fluorescence protein chromophore analogue stabilized by a C = O . . . $\pi$ interaction

ASHISH SINGH, BASANTA KUMAR RAJBONGSHI and GURUNATH RAMANATHAN\*

Department of Chemistry, Indian Institute of Technology Kanpur, Kanpur, India 208 016  
e-mail: gurunath@iitk.ac.in

MS received 10 November 2014; revised 15 January 2015; accepted 25 January 2015

**Abstract.** Crystal structures of four *red kaede* fluorescence protein chromophore analogues are reported here. Molecules I-III adopt a non-planar geometry stabilized by  $\pi \dots \pi$  stacking and hydrogen bonding. Introduction of an electron push-pull system induces molecule IV to be planar and a C = O . . .  $\pi$  supramolecular interaction is observed as well. Strong electron withdrawing and donating groups also ensure formation of a higher order two and three dimensional supramolecular architecture through hydrogen bonds in molecules I and IV. All the analogues exhibit good photoluminescence properties and emit in the red region with excellent quantum yields.

**Keywords.** Imidazolin-5-one; *RFP* chromophore; C = O . . .  $\pi$  stacking; planar polyenes; supramolecular interactions.

## 1. Introduction

*Red kaede* fluorescence protein (*RFP*) belongs to the family of *green fluorescent proteins (GFP)* that were isolated from the stony coral *trachyphyllia geoffroyi*.<sup>1</sup> *Kaede proteins* contain a *GFP* like imidazolin-5-one chromophore. However, on absorption of UV or violet light (350–420nm), the protein backbone between N $_{\alpha}$  and C $_{\alpha}$  of His62 breaks and forms the *red kaede* fluorescent protein chromophore<sup>2</sup> (figure 1). This chromophore is 2000 times more fluorescent in comparison to the wild type *GFP* chromophore. Due to its importance as a fluorescent marker<sup>3</sup> and use in application such as ultra-high resolution fluorescence imaging,<sup>4</sup> this chromophore and its analogues were synthesized and investigated by us. The *kaede* chromophore has also been studied as an organic photovoltaic material.<sup>5</sup> The crystal structures of *kaede* chromophores or its analogues have not yet been studied systematically. The first crystal structure of a *red kaede* protein chromophore analogue was reported by our group in 2012, wherein we observed a deviation from planarity with two distinct orientations of the N-phenyl ring in the molecule that resulted in chiral conformations giving rise to an interesting concomitant polymorphism.<sup>6</sup>

In crystals of *RFP* and many of the *GFP* chromophore analogues, intermolecular interactions, such as O . . . H/C-H . . .  $\pi$  hydrogen bonding<sup>7</sup> and  $\pi \dots \pi$

stacking facilitate the formation of pyramids,<sup>6</sup> layers,<sup>8</sup> sheets<sup>9</sup> and other supramolecular structures.<sup>10</sup> A donor-acceptor type of C=O . . . C short contact in one of the imidazolin-5-one derivatives was reported by our group previously.<sup>9a</sup> Here, in this communication, we show that supramolecular architecture and crystal packing of four *RFP* chromophore analogues (figure 1) can be tailored by appropriate substitutions. These molecules are not planar despite being  $\pi$ -conjugated systems. Conformation of conjugated molecules is a delicate interplay between eclipsing strains of groups around the double bonds, steric effects of the substituents and the counterbalancing electron transfer through the conjugated  $\pi$  bonds. If the former is the stabilizing factor, then the molecule twists out of plane to become curved.<sup>6</sup> Creation of an electron push-pull system forces weak C=O . . .  $\pi$ <sup>11</sup> supramolecular interaction in molecule IV, that in turn, stabilizes planarity and also assists in higher order supramolecular assembly. This interaction was supported by theoretical studies as well. We have also analyzed the photoluminescence properties of all analogues and found good quantum yields with emission in the red region.

## 2. Experimental

### 2.1 Materials

Column chromatography was done in 60–120 and 100–200 mesh particle size silica gel and in neutral alumina.

\*For correspondence

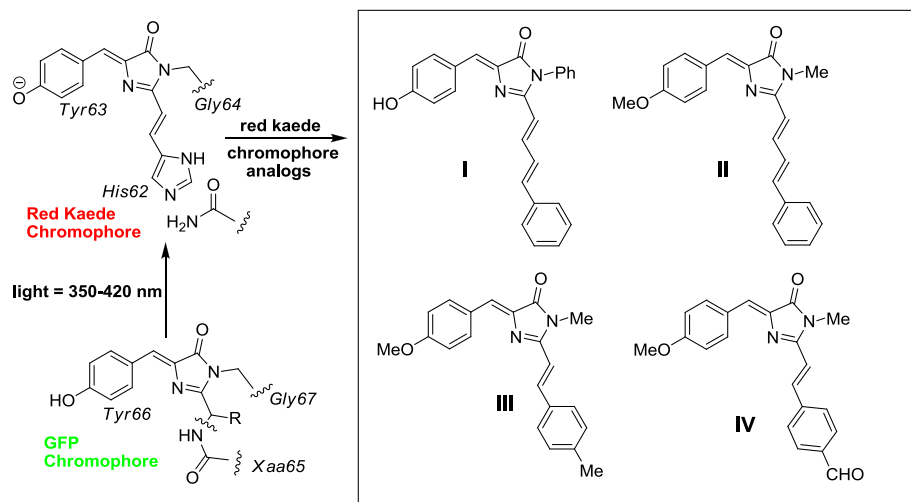


**Figure 1.** Conversion of the *green fluorescent protein* chromophore to a *red kaede* fluorescent protein chromophore (left). The four *red kaede* fluorescent protein chromophore analogues reported here are shown inside the box.

Melting point of all (**I–IV**) compounds was recorded in a JSGW<sup>®</sup> melting point apparatus. For TLC analysis, MERCK<sup>®</sup> Kieselgel 60 F<sub>254</sub> plates were used. <sup>1</sup>H NMR spectra were recorded using JEOL<sup>®</sup> 500 (500 MHz) and JEOL<sup>®</sup> 400 (400 MHz) NMR spectrometer in CDCl<sub>3</sub> as a solvent. Proton decoupled <sup>13</sup>C NMR spectra was taken in JEOL<sup>®</sup> 500 (125 MHz) NMR spectrometer. For recording mass spectra, a Water<sup>®</sup> ESI-Q<sup>tof</sup> instrument was used.

All solvents were purchased from SD Fine Chemicals. These were purified by literature procedures.<sup>12</sup> Anhydrous sodium acetate and anhydrous zinc chloride were used as such. *p*-methoxybenzaldehyde, *p*-methyl benzaldehyde, Methylamine, *pN,N*-dimethylaminobenzaldehyde, *trans* cinnamaldehyde and terephthalaldehyde were purchased from Sigma-Aldrich and used as such. Distilled acetic anhydride was used. Synthesis of *Red Kaede* protein chromophore analogues (**I–IV**) is shown in supporting information (scheme 1 and 2)

## 2.2 Synthesis of Compounds (**I–IV**)

Imidazolin-5-ones (**I–IV**) were synthesized by procedures reported previously<sup>6,8b,9,13</sup> (see [supplementary information](#)). Briefly acetyl glycine was refluxed with a *para*-substituted aromatic aldehyde in acetic anhydride in presence of sodium acetate to get an oxazolone. In the next step the column purified oxazolones were converted into imidazolin-5-ones by solvent free Lewis acid catalysed reaction<sup>14</sup> with primary amines (methylamine, aniline). The column purified 2-methylimidazolin-5-ones were further converted to imidazolin-5-ones with extended conjugation (**I–IV**)

by solvent-free vinylogous condensation reaction<sup>13a</sup> with aldehydes (*p*-tolualdehyde, cinnamaldehyde and terephthalaldehyde).

## 2.3 Spectroscopic characterization

**2.3a (4Z)-4-(4-Hydroxybenzylidene)-1-phenyl-2-((1E,3E)-4-phenylbuta-1,3-dienyl)-1,4-dihydro-5H-imidazolin-5-one (**I**):** Needle-shaped deep red crystals. Isolated yield: 80%; M.p. 213–214°C; R<sub>f</sub> 0.5 (45% Ethyl acetate-Petroleum ether). IR (KBr)  $\nu_{\max}/\text{cm}^{-1}$ : 3064, 1668, 1593, 1500, 1442, 1385. <sup>1</sup>H NMR (500 MHz, CDCl<sub>3</sub>+ DMSO-*D*<sub>6</sub>):  $\delta$  6.18 (d, *J* = 14.9 Hz, 1H), 6.86 (d, *J* = 8.6 Hz, 2H), 7.01 (s, 1H), 7.01–7.16 (m, 2H), 7.26–7.28 (m, 1H), 7.32–7.35 (m, 4H), 7.47–7.57 (m, 5H), 7.74 (dd, *J*<sub>1</sub> = 15.2 Hz, *J*<sub>2</sub> = 10.3 Hz, 1H), 8.18 (d, *J* = 8.6 Hz, 2H). <sup>13</sup>C NMR (CDCl<sub>3</sub>+ DMSO-*D*<sub>6</sub>, 125 MHz):  $\delta$  115.9, 116.9, 125.7, 126.6, 127.0, 127.5, 127.6, 127.7, 128.3, 128.6, 128.7, 129.3, 133.3, 134.4, 136.1, 139.3, 140.3, 156.8, 160.0, 169.0. ESI-MS+ *m/z* Calcd. for C<sub>26</sub>H<sub>21</sub>N<sub>2</sub>O<sub>2</sub> 393.1603 [M+H], found 393.1604.

**2.3b (4Z)-4-(4-methoxybenzylidene)-1-methyl-2-((1E,3E)-4-phenylbuta-1,3-dienyl)-1,4-dihydro-5H-imidazolin-5-one (**II**):** Needle-shaped red crystals. Isolated yield: 40%; M.p. 140–145°C; R<sub>f</sub> 0.5 (40% Ethyl acetate-Petroleum ether). IR (KBr)  $\nu_{\max}/\text{cm}^{-1}$ : 3023, 2930, 2837, 1700, 1663, 1595, 1506, 1449. <sup>1</sup>H NMR (500 MHz, CDCl<sub>3</sub>):  $\delta$  3.28 (s, 3H, NCH<sub>3</sub>), 3.87 (s, 3H, OCH<sub>3</sub>), 6.40 (d, *J* = 15.3 Hz, 1H, CH=CH), 6.98 (d, *J* = 8.9 Hz, 2H, ArH), 7.04 (d, *J* = 5.8 Hz, 2H, ArH), 7.12 (s, 1H, =CHAr), 7.31–7.40 (m, 3H), 7.51 (d, *J* =

8.2 Hz, 2H, ArH), 7.88 (m, 1H), 8.21 (d,  $J = 8.5$  Hz, 2H).  $^{13}\text{C}$  NMR ( $\text{CDCl}_3$ , 125 MHz):  $\delta$  26.6, 55.4, 114.3, 114.4, 116.0, 127.2, 127.3, 127.4, 127.8, 128.9, 129.1, 134.4, 136.3, 140.2, 141.2, 158.6, 161.3, 170.8. ESI-MS+  $m/z$  Calcd. for  $\text{C}_{22}\text{H}_{20}\text{N}_2\text{O}_2$  345.1524 [M+H], found 345.1609.

**2.3c** (4*Z*)-4-(4-methoxybenzylidene)-1-methyl-2-(4-methylstyryl)-1*H*-imidazol-5(4*H*)-one (**III**): Rod-shaped yellow crystals. Isolated yield: 30%; M.p. 125–130°C;  $R_f$  0.5 (40% Ethyl acetate-Petroleum ether). IR (KBr)  $\nu_{\text{max}}/\text{cm}^{-1}$ : 2935, 2839, 1698, 1598, 1510, 1436.  $^1\text{H}$  NMR (500 MHz,  $\text{CDCl}_3$ ): 2.39 (s, 3H, ArCH<sub>3</sub>), 3.32 (s, 3H, NCH<sub>3</sub>), 3.87 (s, 3H, OCH<sub>3</sub>), 6.78 (d,  $J = 15.5$  Hz, 1H, CH=CH), 6.97 (d,  $J = 8.5$  Hz, 2H, ArH), 7.13 (s, 1H, =CHAr), 7.23 (d,  $J = 7.95$  Hz, 2H, ArH), 7.53 (d,  $J = 7.95$  Hz, 2H, ArH), 8.06 (d,  $J = 15.9$  Hz, 1H, CH=CH), 8.21 (d,  $J = 8.5$  Hz, 2H, ArH).  $^{13}\text{C}$  NMR ( $\text{CDCl}_3$ , 125 MHz): 21.6, 26.7, 55.4, 111.8, 114.4, 127.1, 127.8, 128.0, 129.8, 132.6, 134.3, 137.8, 140.7, 140.8, 158.9, 161.3, 171.0. ESI-MS+  $m/z$  Calcd. for  $\text{C}_{21}\text{H}_{20}\text{N}_2\text{O}_2$  333.1524 [M+H], found 333.1605.

**2.3d** 4-((*E*)-2-((*Z*)-4-(4-methoxybenzylidene)-1-methyl-5-oxo-4,5-dihydro-1*H*-imidazol-2-yl)vinyl)benzaldehyde (**IV**): Red needle-shape crystals. Isolated yield: 60%;

M.p. 165–170°C;  $R_f$  0.5 (50% ethyl acetate-petroleum ether). IR (KBr)  $\nu_{\text{max}}/\text{cm}^{-1}$ : 3451, 2933, 1688, 1627, 1598, 1463.  $^1\text{H}$  NMR (500 MHz,  $\text{CDCl}_3$ ): 3.34 (s, 3H, NCH<sub>3</sub>), 3.87 (s, 3H, OCH<sub>3</sub>), 6.96 (d,  $J = 16.03$  Hz, 1H, CH=CH), 6.98 (d,  $J = 9.12$  Hz, 2H, ArH), 7.19 (s, 1H, =CHAr), 7.78 (d,  $J = 8.015$  Hz, 2H, ArH), 7.93 (d,  $J = 8.015$  Hz, 2H, ArH), 8.10 (d,  $J = 16.03$  Hz, 1H, CH=CH), 8.21 (d,  $J = 8.5$  Hz, 2H, ArH), 10.04 (s, 1H, CHO).  $^{13}\text{C}$  NMR ( $\text{CDCl}_3$ , 125 MHz):  $\delta$  26.8, 55.5, 114.5, 116.0, 127.5, 128.4, 128.7, 130.3, 134.6, 137.0, 137.4, 138.9, 140.9, 158.0, 161.7, 170.6, 191.4. ESI-MS+  $m/z$  Calcd. for  $\text{C}_{28}\text{H}_{38}\text{N}_3\text{O}$ : 347.13510 [M+H], found 347.1390

#### 2.4 X-ray crystallography

Single crystal X-ray data were collected at 298 K on a Bruker AXS SMART APEX CCD diffractometer equipped with a molybdenum sealed tube ( $\lambda = 0.71073$  Å) and highly oriented graphite monochromator. The data integration and reduction were processed with SAINT+.<sup>15</sup> The collected reflection data were corrected by empirical absorption correction method with SADABS.<sup>16</sup> The structures were solved using WinGX version 1.70.01 package. Direct method using SHELX 97<sup>17</sup> was used for solving the structures. The structures were further refined using full matrix least square

**Table 1.** Summary of x-ray structure parameters of molecules I–IV.

Molecule	I	II	III	IV
Empirical Formula	$\text{C}_{26}\text{H}_{20}\text{N}_2\text{O}_2$	$\text{C}_{22}\text{H}_{20}\text{N}_2\text{O}_2$	$\text{C}_{22}\text{H}_{24}\text{N}_2\text{O}_{2.5}$	$\text{C}_{21}\text{H}_{18}\text{N}_2\text{O}_3$
Molecular Weight	392.44	344.40	356.43	346.37
Temperature/K	298(2)	298(2)	298(2)	298(2)
Crystal system	Monoclinic	Monoclinic	Triclinic	Monoclinic
Space group	$P2_1$	$P2_1/n$	$P-1$	$Pn$
$a/\text{Å}$	6.691(2)	14.121(5)	7.0564(17)	4.9084(17)
$b/\text{Å}$	19.642(4)	10.361(4)	7.4268(17)	14.926(5)
$c/\text{Å}$	7.719(3)	14.130(5)	18.270(4)	12.013(4)
$\alpha/^\circ$	90	90	90.823(5)	90
$\beta/^\circ$	92.123(2)	117.632(7)	91.860(5)	99.761(7)
$\gamma/^\circ$	90	90	109.877(3)	90
Volume/ $\text{Å}^3$	1013.8(5)	1831.5(12)	899.6(4)	867.4(5)
$Z$	2	4	2	2
$D_x/\text{Mg cm}^{-3}$	1.286	1.249	1.316	1.326
$\mu/\text{mm}^{-1}$	0.082	0.081	0.086	0.090
$F(000)$	412	728	380	364
Crystal size / Mm	0.27×0.22×0.20	0.24×0.21×0.19	0.22×0.19×0.18	0.16×0.14×0.13
$\theta$ range for data collection <sup>0</sup>	2.1–28.4	2.5–28.3	3.1–25.5	2.2–26
Reflections collected	6471	11792	4916	7682
Independent reflections	3803	4499	3277	2880
Data/restraints/ parameters	3803/1/ 271	4499/0/ 235	3277/1/ 249	2880/2/ 235
Goodness-of-fit on $F^2$	1.056	0.954	1.022	1.028
Final $R$ indices [ $I > 2\text{Sigma}(I)$ ]	$R1 = 0.0936$ $wR2 = 0.2105$	$R1 = 0.0626$ $wR2 = 0.2079$	$R1 = 0.0769$ $wR2 = 0.2519$	$R1 = 0.0536$ $wR2 = 0.1565$
CCDC No.	<b>951962</b>	<b>951960</b>	<b>951961</b>	<b>951959</b>

**Table 2.** Significant intermolecular interactions (interatomic distances in Å and bond angles in °) observed in the crystal structures of imidazolin-5-ones I–IV.

Molecule	D-H...A	D-H (Å)	H...A (Å)	D...A (Å)	<D-H...A(°)	Symmetry codes
<b>I</b>	O(2)-H(2)...O(1)	0.82	1.91(40)	2.671(60)	153(33)	$-x, -0.5+y, 2-z$
	C(17)-H(17)...O(2)	0.93	2.67(47)	3.231(80)	119(41)	$2-x, 1/2+y, 1-z$
<b>II</b>	C(16)-H(16)...O(1)	0.93	2.67 (18)	3.557(32)	159(18)	$0.5-x, 0.5+y, 1.5-z$
<b>III</b>	C(4)-H(4)...O(1)	0.93	2.41(30)	3.257(45)	152(21)	$1-x, -y, 1-z$
	C22-H(22A)...O(1)	0.96	2.14(27)	2.877(32)	169(33)	$1-x, -y, 1-z$
<b>IV</b>	C(21)-H(21C)... $\pi$	0.96	2.68(5)	3.562(32)	152(22)	$1+x, 1+y, z$
	C(3)-H(3)...O(2)	0.93	2.40 (26)	3.315(5)	168(12)	$-2+x, y, 1+z$

on  $F^2$  (SHELX 97).<sup>17</sup> All the non-hydrogen atoms were refined anisotropically. The hydrogen atoms were refined isotropically and treated as riding atoms by using SHELXL default parameters. The structures reported here have been deposited in CCDC database and have the accession numbers **951959-62**.

### 3. Results and Discussion

#### 3.1 Crystallographic studies

All crystals were grown by slow evaporation from a 3:1 mixture of methanol and dichloromethane at room temperature. Molecules **I**, **II** and **IV** crystallized in monoclinic system, while molecule **III** crystallized in a triclinic crystal system. The ortep diagrams of all the reported molecules are shown in supporting

information (figure S1). Crystallographic parameters of molecule **I–IV** are given in table 1 and significant intermolecular interactions are summarized in the table 2.

Molecule **I** crystallized in a monoclinic system with chiral space group  $P2_1$  (table 1). The mono-substituted benzene ring and *p*-disubstituted benzene ring twist out of the imidazolin-5-one plane by 2° and 8° respectively. The crystal structure of molecule **I** exhibits a strong hydrogen bond between O(2)-H(2)...O(1) of the imidazolin-5-one ring with a distance of 1.91 Å and associated bond angle is 152.8°. A stable  $\pi$ ... $\pi$  stacking<sup>18</sup> with a distance of 3.58 Å between imidazolin-5-one and mono-substituted benzene ring is also present. The hydrogen bonding interaction and  $\pi$ ... $\pi$  stacking assembles into a two-dimensional sheet-like supramolecular architecture in molecule **I** (figure 2).

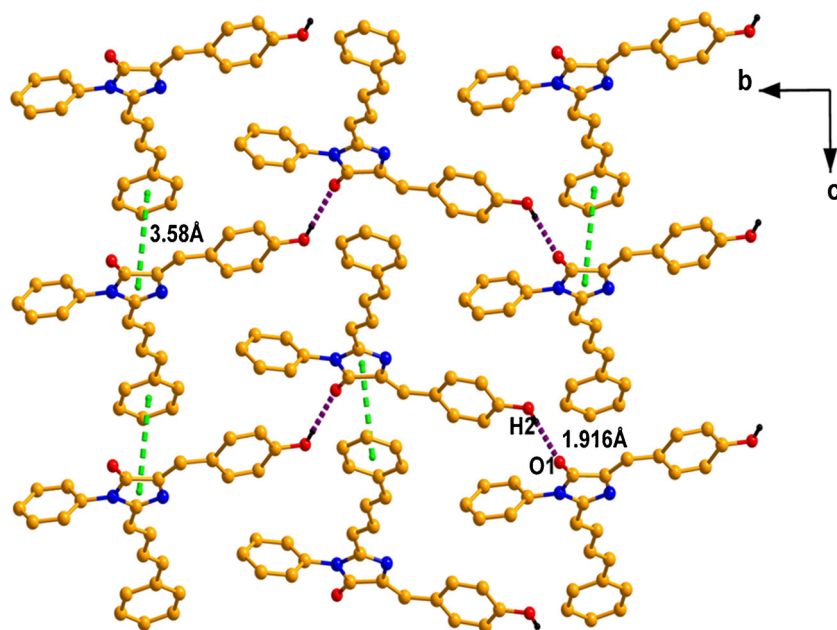


**Figure 2.** Two dimensional sheet in molecule **I** formed by O(2)-H(2)...O(1) hydrogen bond (1.91 Å, dotted violet line) and  $\pi$ ... $\pi$  stacking (3.58 Å, dotted green line). Some of the hydrogen atoms are omitted for clarity. Colour code: carbon: yellow; oxygen: red; nitrogen: blue; hydrogen: black.

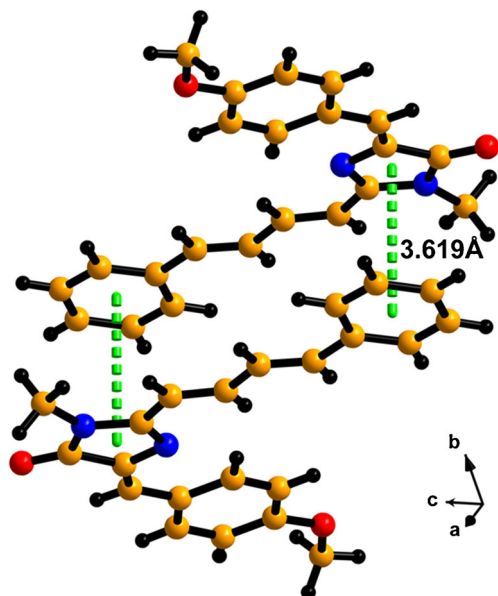


**Figure 3.** A  $\pi\cdots\pi$  stacking between imidazolin-5-one and monosubstituted benzene ring (green dotted line) in molecule **II**. Colour code: carbon: yellow; oxygen: red; nitrogen: blue; hydrogen: black.

Molecule **II** was also crystallized in monoclinic crystal system but in achiral space group  $P2_1/n$ . The unit cell contains four molecules. Molecule **II** also deviates significantly from planarity. The two benzene rings are rotated by  $8^\circ$  and  $5^\circ$  from the imidazolinone-5-one ring plane respectively. The crystal structure shows a weak  $\pi\cdots\pi$  stacking between the electron deficient imidazolin-5-one heterocyclic ring and the mono-substituted benzene ring with a distance  $3.61 \text{ \AA}$  (figure 3). A weak intermolecular hydrogen bond is formed between imidazolinone oxygen O(1) and aromatic hydrogen C(16)-H(16) ( $2.67 \text{ \AA}$ ), which is shorter than the sum of the van der Waals radii of the interacting atoms. This weak hydrogen bond makes the molecules arrange themselves in a zig-zag fashion to form a one-dimensional chain-like structure (figure S2).

Molecule **III** crystallized in a triclinic crystal system with centrosymmetric space group  $P-1$ . The asymmetric unit of molecule **III** contains two solvent (methanol) molecules. Both the methanol molecules appear at the edge of the unit cell (figure S3) and have a statistical

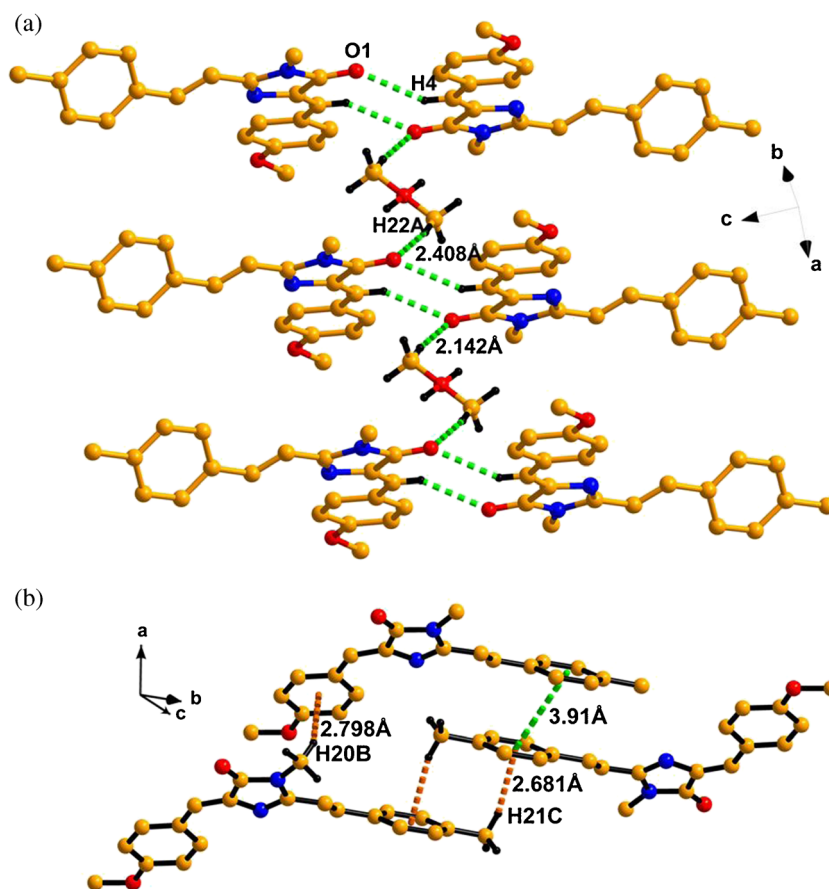


**Figure 4.** (a) Layer structure of molecule **III** formed by C(4)-H(4) $\cdots$ O(1) and C(22)-H(22A) $\cdots$ O(1) hydrogen bonds (dotted green lines); (b) C(21)-H(21C) $\cdots\pi$  hydrogen bonds (dotted orange lines) and  $\pi\cdots\pi$  stacking (green dotted line) between molecules. Some of the hydrogen atoms are omitted for clarity. Colour code: carbon: yellow; oxygen: red; nitrogen: blue; hydrogen: black.

disorder. The *p*-methyl substituted benzene ring is significantly twisted and results in a  $44^\circ$  deviation from the plane of imidazolin-5-one ring. The dihedral angle between *p*-methoxy substituted benzene and imidazolinone ring is  $4^\circ$ . The molecules form a sheet like structure with the help of intermolecular C(4)-H(4) $\cdots$ O(1) (2.41 Å) hydrogen bonds while the methanol molecules form individual C(22A)-H(22A) $\cdots$ O(1) (2.14 Å) hydrogen bonds between the sheets, thus connecting the layers (figure 4b). A weak  $\pi\cdots\pi$  stacking (3.91Å) is observed between the two *para* substituted benzene rings. Apart from  $\pi\cdots\pi$  stacking, two C-H $\cdots\pi$  hydrogen bonds (C-H(20B) $\cdots\pi$  (2.798 Å) and CH(21C) $\cdots\pi$  (2.681Å)) are also present which stabilize the molecular packing (figure 4b).

Molecule **IV**, which has a free aldehyde group at the *para* position of the benzene ring, adopted a planar  $\pi$ -skeleton. The molecule **IV** crystallized with the *Pn* space group. The dihedral angle of the aldehyde containing benzene and *para* methoxy substituted benzene ring with imidazolinone ring is  $1^\circ$  and  $3^\circ$  respectively. The molecular architecture is stabilized by two intermolecular hydrogen bonds (between C(3)-H(3) $\cdots$ O(2) (2.40 Å,  $167.5^\circ$ ) and C(17)-H(17) $\cdots$ O(3) (2.63 Å,  $133.5^\circ$ )). Moreover, apart from hydrogen bonds, a striking C=O $\cdots\pi$  interaction is observed between

C(21)-O(2) $\cdots\pi$  with the distance of 3.35Å (figure 5). This distance is shorter than the sum of van der Waals radii of the interacting atoms.<sup>19</sup> The nature of the C=O $\cdots\pi$  interaction is most likely a lone pair $\cdots\pi$  interaction. The hydrogen bonds and C=O $\cdots\pi$  interactions holds this molecule in three dimensions and forms a supramolecular network of molecule **IV**. The C=O $\cdots\pi$  interaction thus mandates planarity as a stereoelectronic requirement. The C=O $\cdots\pi$  interactions thus play a significant role in stabilizing the planarity in molecule **IV**.

The C=O $\cdots\pi$  interaction in *RFP* chromophore (molecule **IV**) was further investigated by electronic structure theory. The wave functions were generated by applying B3LYP approximations using 6-31G(d,p)<sup>20</sup> basis set for the supramolecular interactions of the crystal structure of molecule **IV**. These calculations were analyzed by AIMALL software<sup>21</sup> in light of Bader's theory<sup>22</sup> of atom in molecules. The electron density distribution in the crystal environment supports the presence of C=O $\cdots\pi$  interactions. A bond critical point of spatial electron density of (3, -1) nature is found in molecule **IV** between oxygen of free CHO and the electron deficient benzene ring (figure S4). Also the positive value for the laplacian<sup>22</sup> ( $\rho_{\text{bcp}}$ ) supports a closed shell C=O $\cdots\pi$  interaction (figure S4)

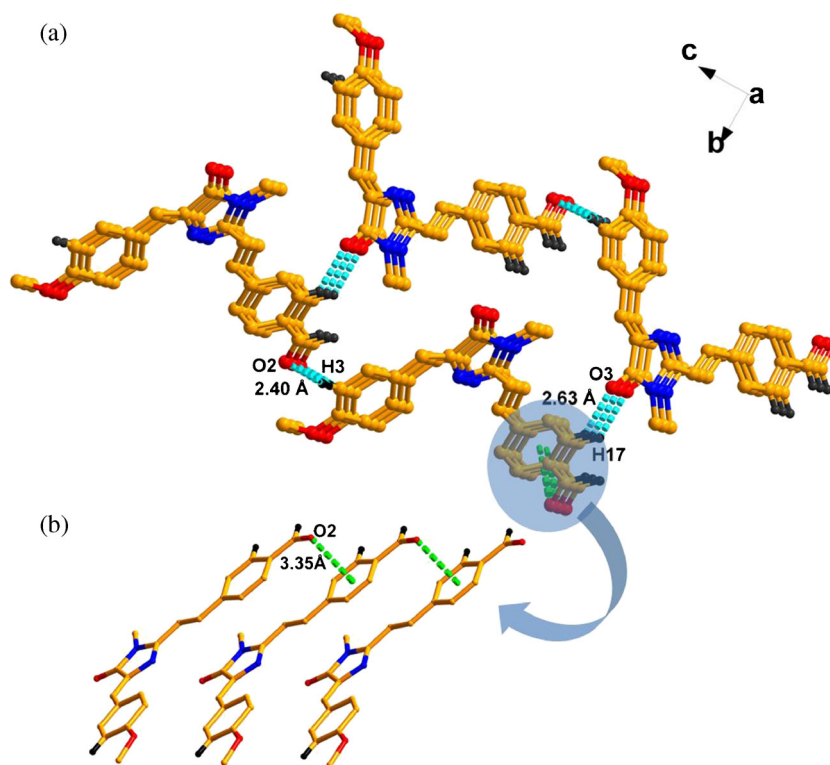


**Figure 5.** (a) Three dimensional arrangement of molecule **IV** stabilized by C-H $\cdots$ O hydrogen bonding and C=O $\cdots\pi$  interactions. (b) A close view of C=O $\cdots\pi$  interactions. Other hydrogen atoms are free from short contact and are omitted for clarity. Colour code: carbon: yellow; oxygen: red; nitrogen: blue; hydrogen: black.

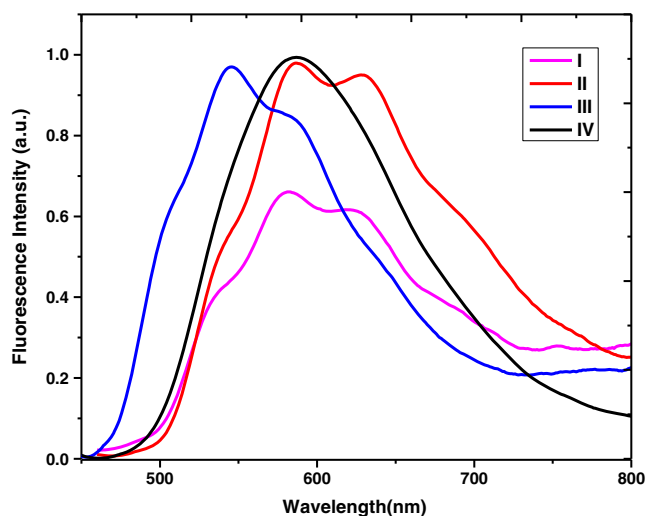


**Figure 6.** Normalized emission spectra of molecule **I–IV** at room temperature in methanol solvent (Excitation wavelength: 441 nm for **I** and **II**, 426 nm and 431 nm for molecule **III** and **IV** respectively).

The *RFP* chromophore analogues are supposed to have a planar structure due to the  $sp^2$  hybridized skeleton. However molecules **I–III** and the previously reported *N*-phenyl analogue<sup>6</sup> adopted a non-planar geometry, stabilized by hydrogen bonding,  $\pi\cdots\pi$  stacking and C–H $\cdots\pi$  hydrogen bonds type of supramolecular interaction. Molecule **IV**, where a strong electron withdrawing group (-CHO) is present adopted a planar structure stabilized only through the hydrogen bond and C=O $\cdots\pi$  interactions. Among all the known *RFP* chromophore analogues till date, molecule **IV** is the first example having the C=O $\cdots\pi$  interaction and a planar structure.

The photophysical properties of molecule **I–IV** have been investigated in methanol in 10  $\mu$  M concentrations and data is presented in table S1. All molecules give absorption maximum in a 20 nm range ( $\lambda_{\max} = 426\text{--}441$  nm) (figure S5). Molecules **I** and **II** absorb and emit at longer wavelength because of extra conjugation as compared to molecule **III** and **IV** (figure 6). The value of molar extinction coefficient of molecule **IV** is the highest (amongst those reported here) and shows a strong electron delocalization in this molecule<sup>23</sup> due to planarity. Molecule **IV** has a high quantum yield (0.029) due to the presence of strong donor-acceptor group in the molecule.

#### 4. Conclusion

We report a series of crystal structures of the *red kaede* fluorescent protein chromophore analogues. We show that molecules **I** to **III** deviate from planarity while molecule **IV** adopt a planar structure. A C=O $\cdots\pi$

supramolecular interaction is present in molecule **IV** that facilitates electron donation from the methoxy group across the  $\pi$ -skeleton of the molecule to the aldehyde group. In all the molecules,  $\pi\cdots\pi$  stacking is present while a strong hydrogen bonding is observed in molecule **I** to stabilize the crystal packing. We also noticed that the presence of strong electron donating groups (-OH in molecule **I**) and electron withdrawing group (-CHO in molecule **IV**) leading to two and three dimensional supramolecular architecture respectively. This creation of electron pushpull systems forces the molecule to become planar in order to ensure that the *p*-orbitals are aligned to facilitate electron transfer across the molecule which is also supported by photophysical studies. Further investigations in this regard are under way.

#### Supplementary Information

Supplementary information contains spectra of all compounds and are available at [www.ias.ac.in/chemsci](http://www.ias.ac.in/chemsci).

#### Acknowledgements

We are thankful to IIT, Kanpur, India for the financial assistance and Mr. Khalid Badi-Uz-Zama for assisting us in computational study. A.S. and B.K.R. thank UGC and CSIR, India for junior and senior research fellowship (JRF & SRF). Compound **I** was synthesized and solved by B.K.R. and has been reported only in his thesis previously. At present, B.K.R. is an assistant professor at Cotton College State University, Assam. Anonymous referees are thanked for their comments.

#### References

- Ando R, Hama H, Yamamoto-Hino M, Mizuno H and Miyawaki A 2002 *PNAS* **99** (20) 12651
- (a) Mizuno H, Mal T K, Tong K I, Ando R, Furuta T, Ikura M and Miyawaki A 2003 *Molecular Cell* **12** 1051; (b) Hayashi I, Mizuno H, Tong K I, Furuta T, Tanaka F, Yoshimura M, Miyawaki A and Ikura M 2007 *J. Mol. Biol.* **372** 918; (c) Yampolsky I V, Kislukhin A A, Amatov T T, Shcherbo D, Potapov V K, Lukyanov S and Lukyanov K A 2008 *Bioorganic Chemistry* **36** 96
- (a) Lippincott-Schwartz J, Altan-Bonnet N and Patterson G H 2003 *Nat. Cell Biol.* **S7**; (b) Wiedenmann J, Ivanchenko S, Oswald F, Schmitt F, Rocker C, Salih A, Spindler K-D and Nienhaus G U 2004 *PNAS* **101** 15905; (c) Sato T, Takahoko M and Okamoto H 2006 *Genesis* **44** 136
- Betzig E, Patterson G H, Sougrat R, Lindwasser O W, Olenych S, Bonifacino J S, Davidson M W, Lippincott-Schwartz J and Hess H F 2006 *Science* **313** 1642
- (a) Jain V, Rajbongshi B K, Mallajosyula A T, Bhattacharjya G, Iyer S S K and Ramanathan G 2008

- Sol. Energy Materials Sol. Cells* **92** 1043; (b) Chuang W-T, Chen B-S, Chen K-Y, Hsieh C-C and Chou P-T 2009 *Chem. Commun.* 6982
6. Rajbongshi B K, Nair N N, Nethaji M and Ramanathan G 2012 *Cryst. Growth Des.* **12** 1823
  7. Nishio M, Umezawa Y, Honda K, Tsuboyama S and Suezawa H 2009 *Cryst. Eng. Comm.* **11** 1757
  8. (a) Singh A, Rajbongshi B K and Ramanathan G 2014 *J. Chem. Sci.* **126** (5) 1275; (b) Rajbongshi B K and Ramanathan G 2009 *J. Chem. Sci.* **121** (6) 973
  9. (a) Bhattacharjya G, Savitha G and Ramanathan G 2004 *CrystEngComm* **6** (40) 233; (b) Bhattacharjya G, Savitha G and Ramanathan G 2005 *J. Mol. Struct.* **752** 98
  10. (a) Leininger S, Olenyuk B and Stang P J 2010 *Chem. Rev.* **100** 853; (b) Desiraju G R 1989 *Crystal Engineering: The design of Organic* (Amsterdam: Elsevier)
  11. (a) Addadi L and Lahav M 1979 *Pure Appl. Chem.* **39** 1269; (b) Moorthy J N, Samant S D and Venkatesan K 1994 *J. Chem. Soc. Perkin Trans.* **2** 1223; (c) Yang X, Wu D, Ranford J D and Vittal J J 2005 *Cryst. Growth Des.* **5** (1) 41; (d) Drew M G B, De S, Nag S and Datta D 2009 *Inorg. Chim. Acta* **362** 610; (e) Gao X-L, Lu L-P and Zhu M-L 2009 *Acta Cryst.* **C65** o123; (f) Gautrot J E, Hodge P, Cupertino D and Helliwella M 2006 *New J. Chem.* **30** 1801
  12. Armarego W L F and Perrin D D 1997 In *Purification of Laboratory Chemicals*. 4th edition (Oxford: Butterworth-Heinemann)
  13. (a) Bhattacharjya G, Agasti S S and Ramanathan G 2006 *ARKIVOC* x 152; (b) Yang J-S, Huang G-J, Liu Y-H and Peng S-M 2008 *Chem. Commun.* 1344; (c) Hoshina H, Tsuru H, Kubo K, Igarashi T and Sakurai T 2000 *Heterocycles* **53** 2261
  14. Tanaka K and Toda F 2000 *Chem. Rev.* **100** 1025
  15. SAINT+ version 6.02 [M], Bruker AXS, Inc.: Madison WI **1999**
  16. Sheldrick G M SADABS: Empirical Absorption Correction Program; University of Göttingen: Göttingen, Germany **1997**
  17. Sheldrick G M SHELXS97 and SHELXL97, Programs for Crystal Structure Analysis (Release 97-2), University of Göttingen, Germany 1997
  18. (a) Hunter C A and Sanders J K M 1990 *J. Am. Chem. Soc.* **112** (14) 5525; (b) Cozzi F, Cinquini M, Annuziata R and Siegel J S 1993 *J. Am. Chem. Soc.* **115** 5330
  19. Zhang Z, Tong H, Wu Y and Zhang G 2012 *New J. Chem.* **36** 44
  20. (a) Ditchfield R, Hehre W J and Pople J A 1971 *J. Chem. Phys.* **54** 724; (b) Hehre W J, Ditchfield R and Pople J A 1972 *J. Chem. Phys.* **56** 2257
  21. Keith T A, Software T K G and KS O P 2014 *USA* Version 14.04.17 edn
  22. Bader R F W 1990 In *Atoms in Molecules: A Quantum Theory* (UK: Oxford University)
  23. Christensen M K, Jennum K, Abrahamsen P B, Pia E A D, Lincke K, Broman S L, Nygaard D B, Bond A D and Nielsen M B 2012 *RSC Advances* **2** 8243